Supporting Information for

Solvent- and Base-Free Synthesis of Wax Esters from Fatty Acid Methyl Esters by Consecutive One-Pot, Two-Step Catalysis.

D. H. Nguyen,[a] G. Raffa,[a] Y. Morin,[a] S. Desset,[a] F. Capet,[a] V. Rataj,[a] F. Dumeignil*[a], R. M. Gauvin*[a]

[a] *Univ. Lille, CNRS, Centrale Lille, ENSCL, Univ. Artois, UMR 8181 - UCCS - Unité de Catalyse et Chimie du Solide, F-59000 Lille, France.*

* Corresponding authors: Franck.Dumeignil@univ-lille1.fr, Regis.Gauvin@ensc-lille.fr

Table of contents

1. NMR characterization of complex 3.

Figure S1. ^{1}H NMR spectrum of **3** (C_6D_6, 300K).

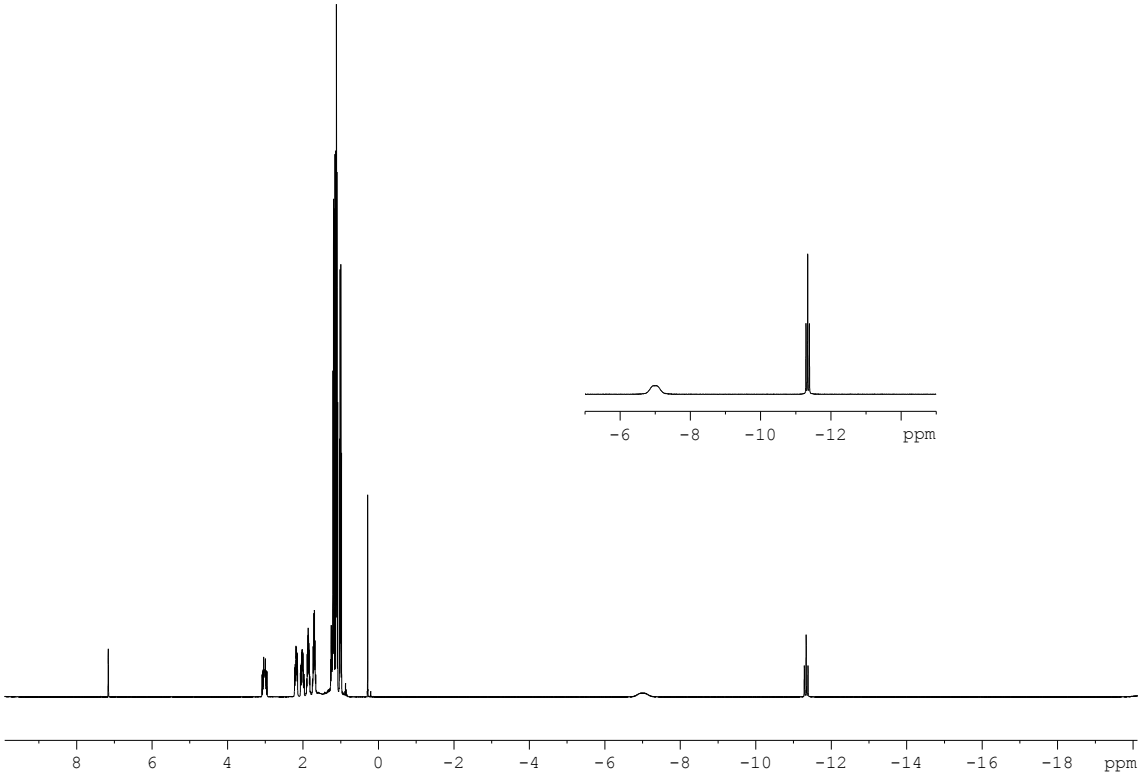

Figure S2. $^{1}H\{^{31}P\}$ NMR spectrum of **3** (C_6D_6, 300K).

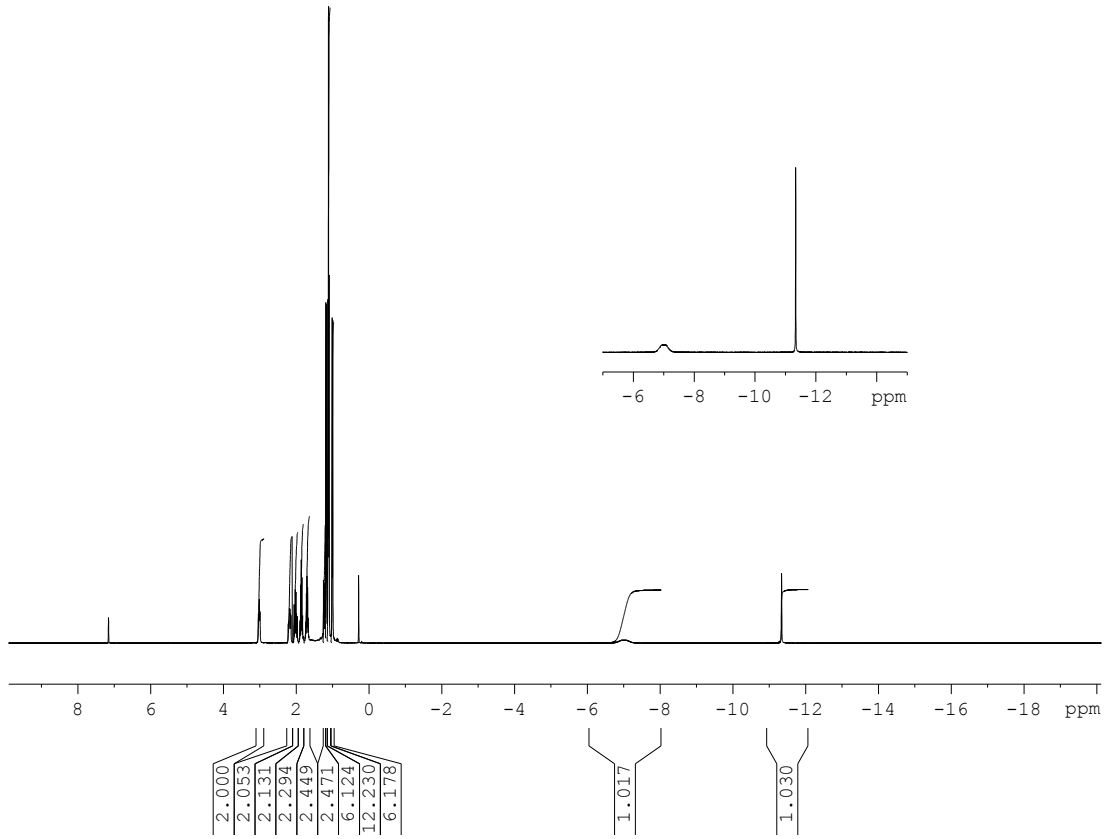

Figure S3. $^{31}P\{^{1}H\}$ NMR spectrum of **3** (C_6D_6, 300K).

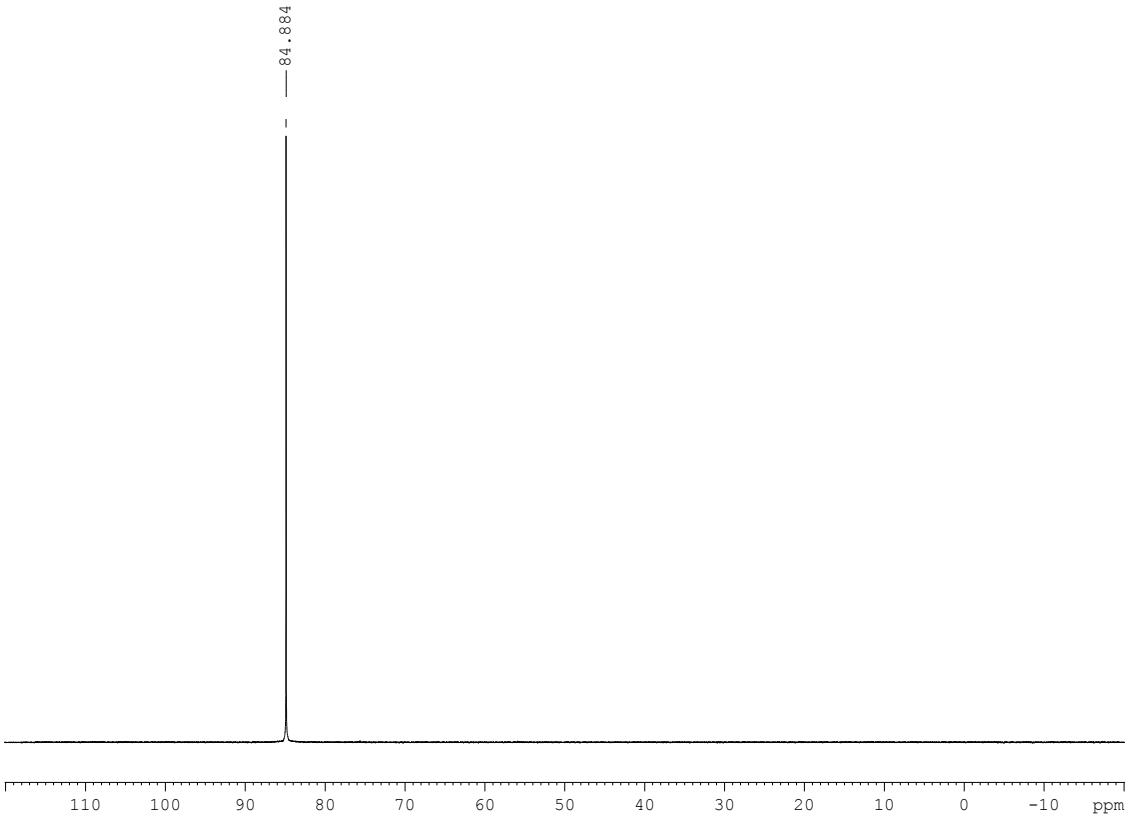

Figure S4. $^{11}B\{^{1}H\}$ NMR spectrum of **3** (C_6D_6, 300K).

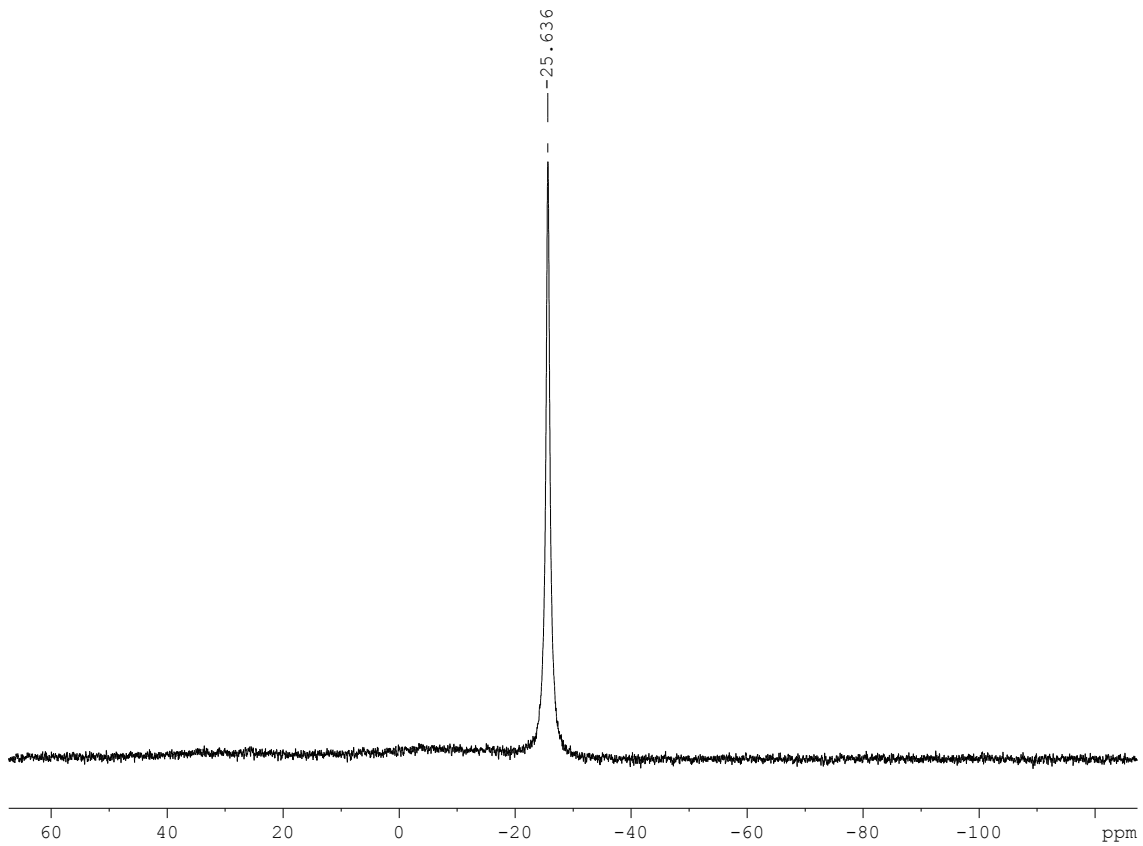

Figure S5. ^{1}H-^{15}N HSQC NMR spectrum of **3** (C_6D_6, 300K).

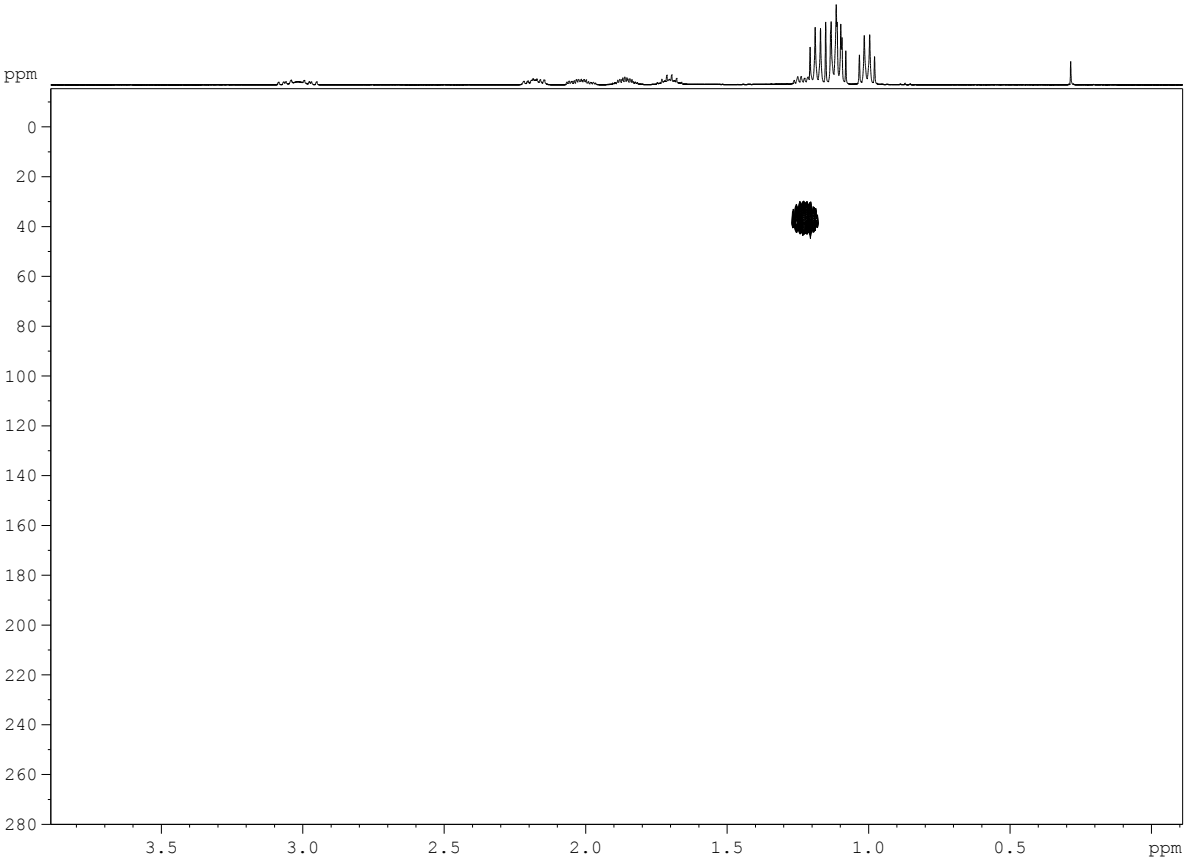

Figure S6. $^{13}C\{^{1}H\}$ JMOD NMR spectrum of **3** (C_6D_6, 300K).

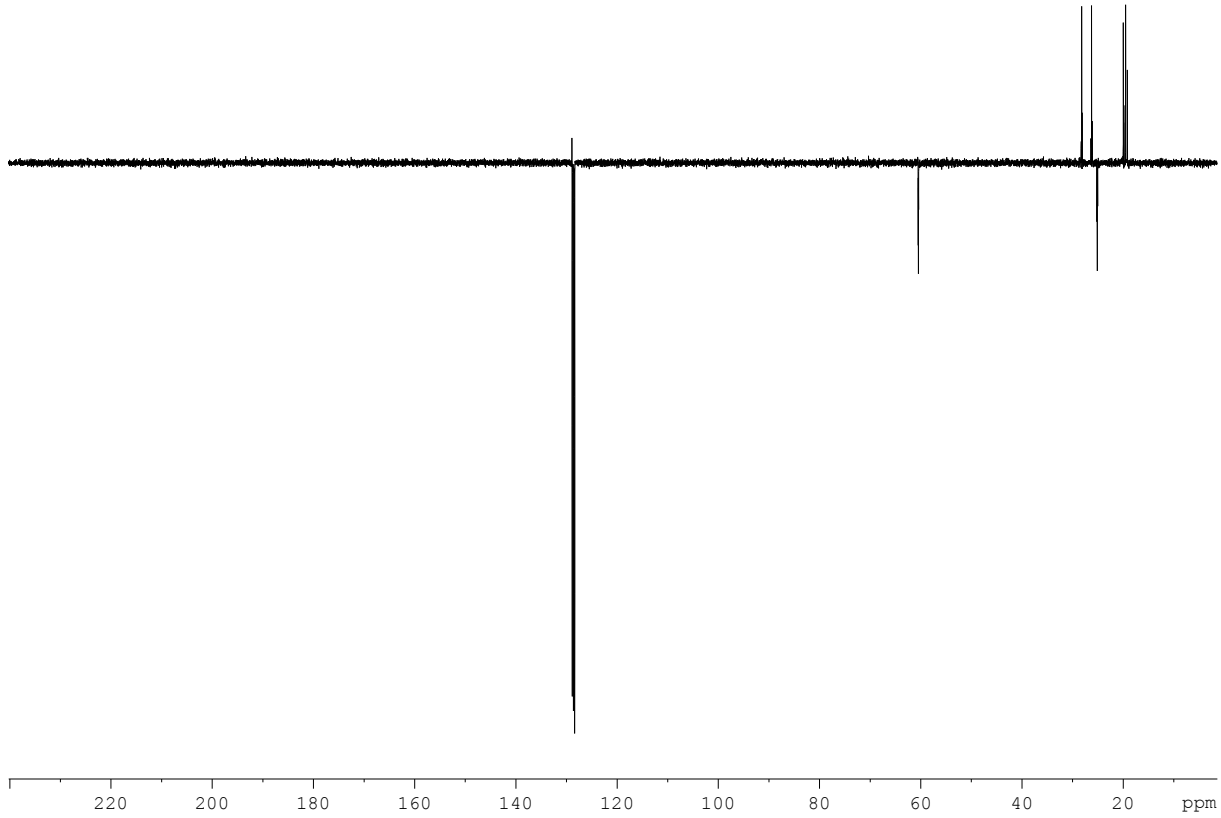

Figure S7. ^{1}H-^{13}C HSQC-TOCSY NMR spectrum of **3** (C_6D_6, 300K).

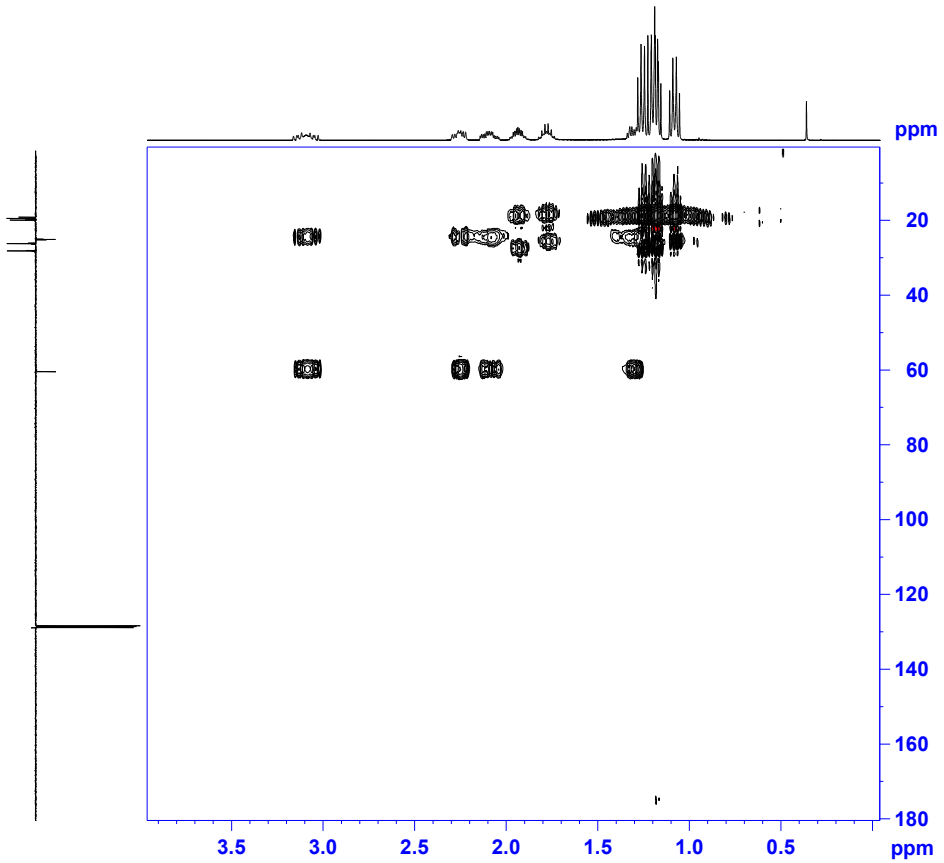

Figure S8. ^{1}H-^{13}C HSQC NMR spectrum of **3** (C_6D_6, 300K).

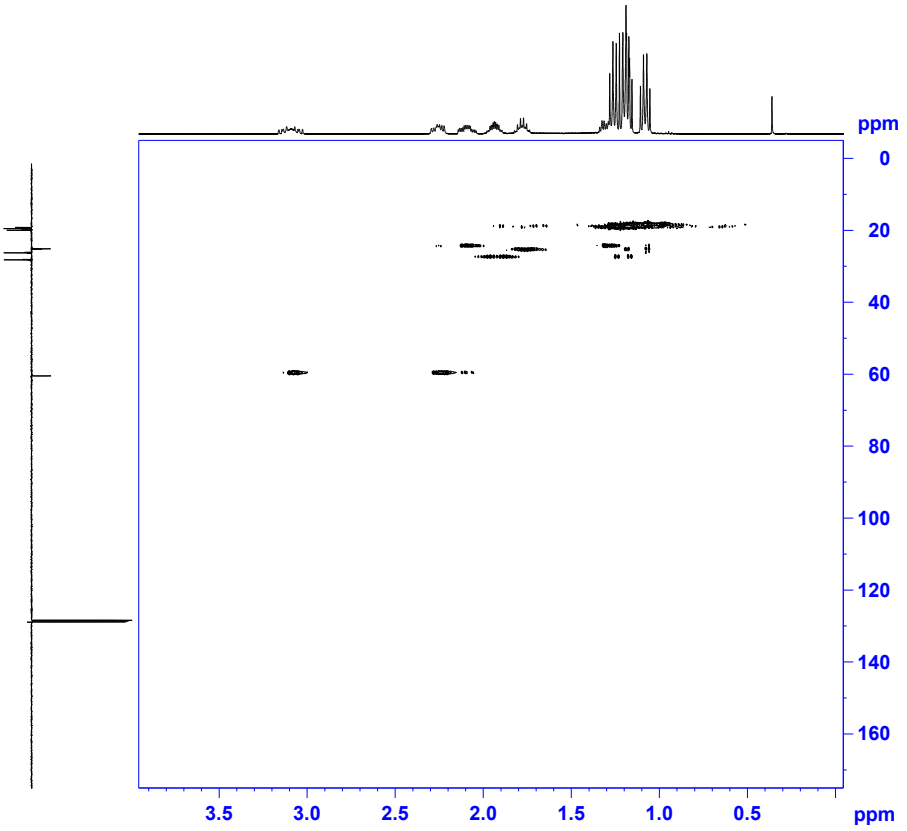

Figure S9. ^{1}H-^{1}H COSY NMR spectrum of **3** (C_7D_8, 225K)

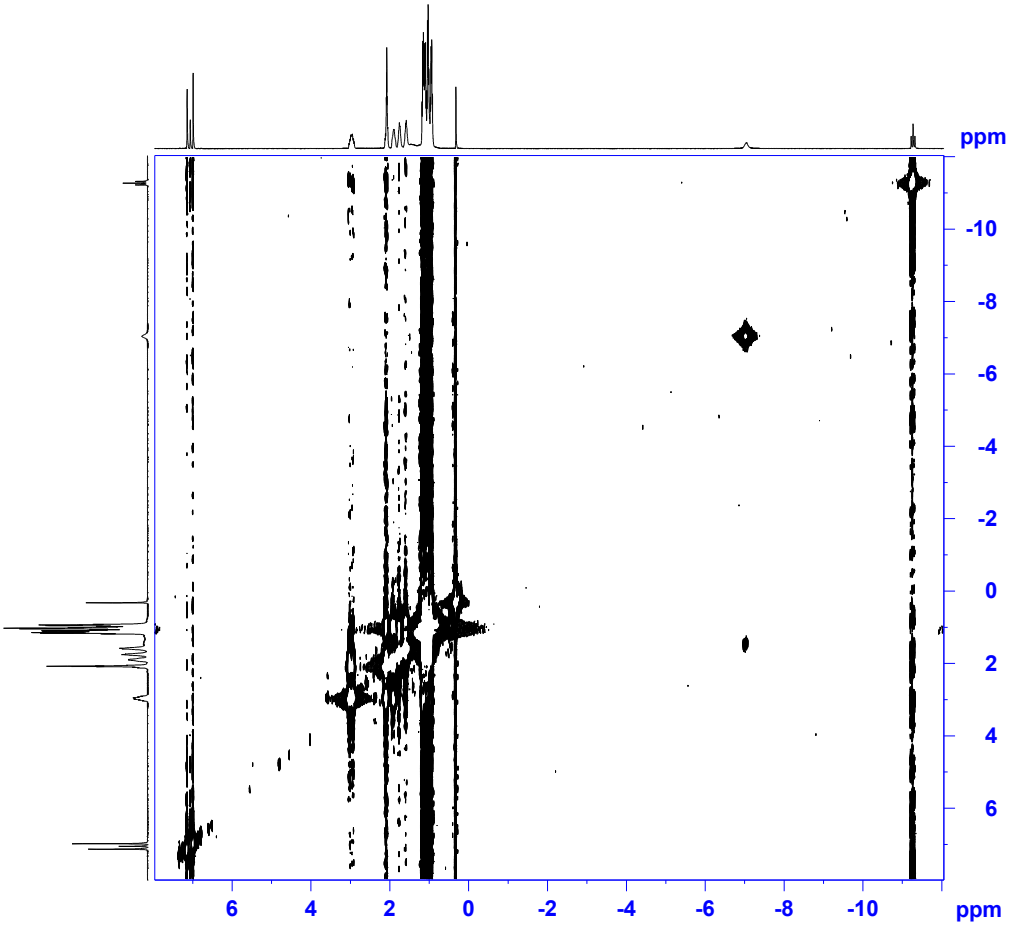

2. Kinetic studies for the formation of 3.

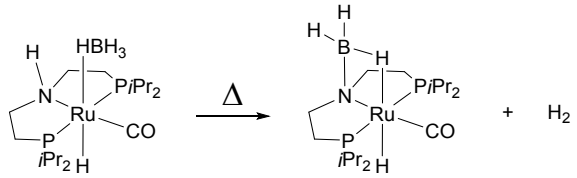

2 **3**

Figure S10. Stacked ^{1}H NMR spectra at 343K.

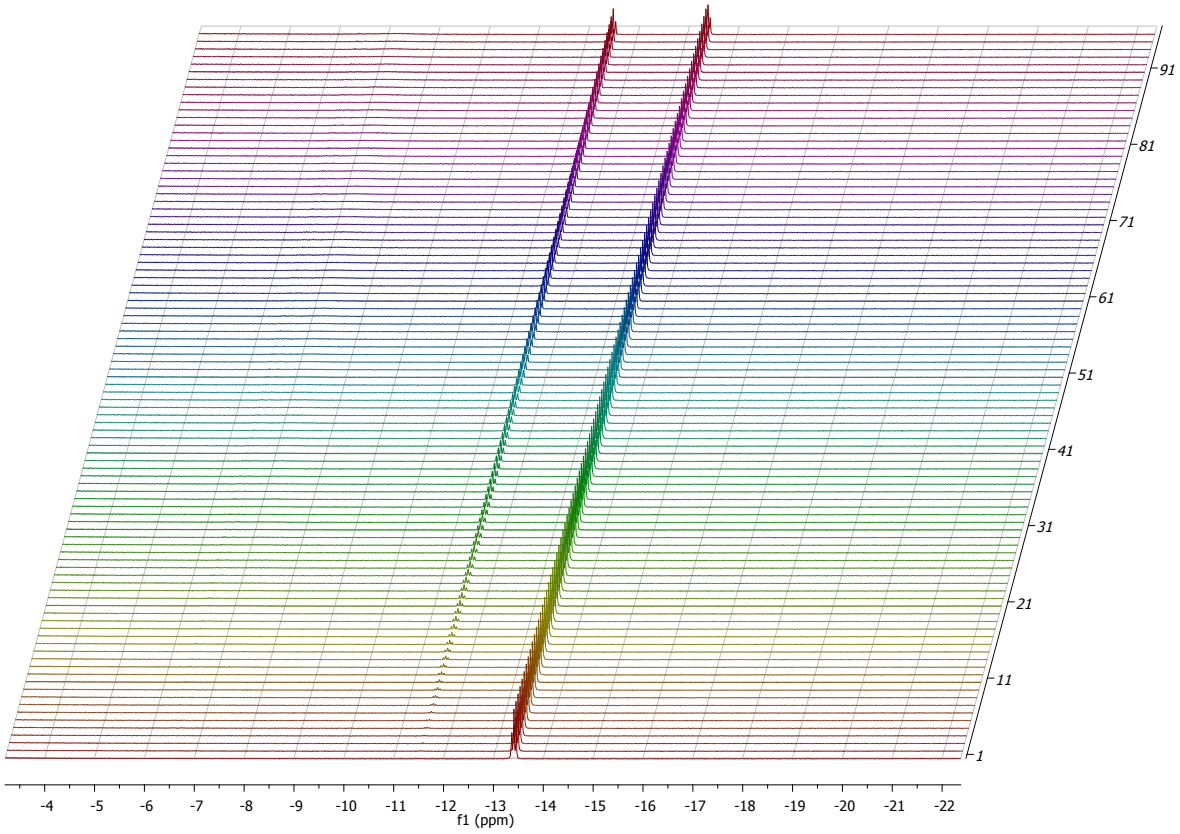

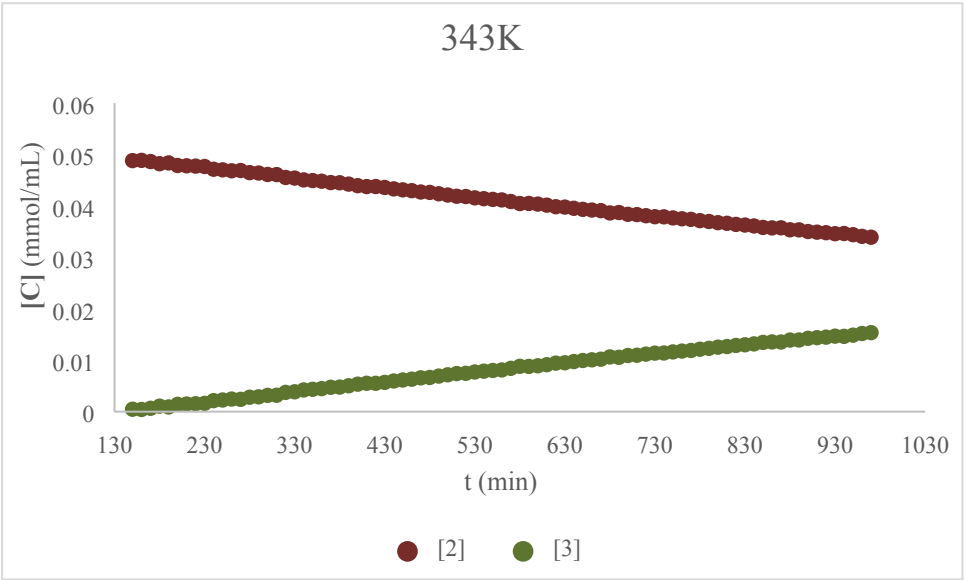

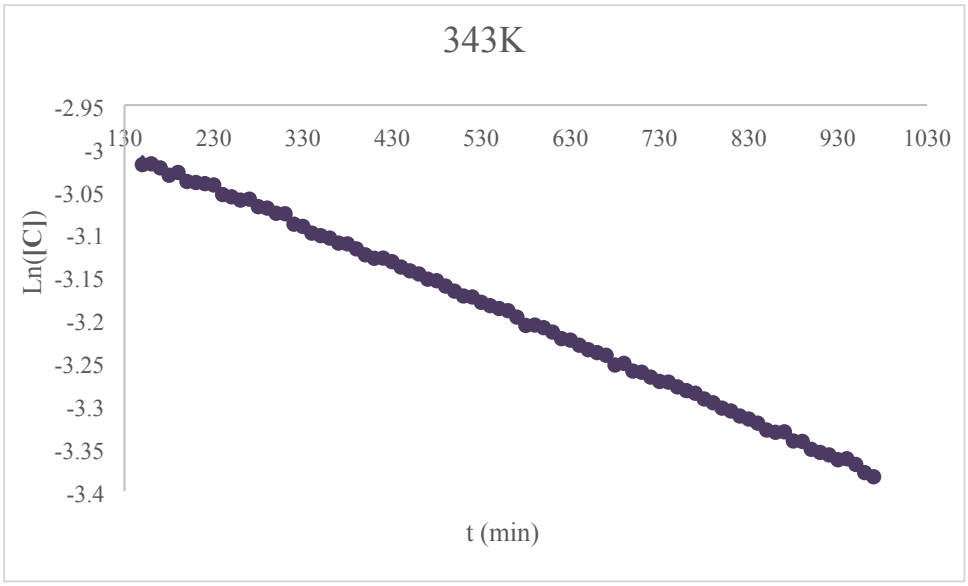
343K
-2.95
-3
-3.05
-3.1
-3.15
-3.2
-3.25
-3.3
-3.35
-3.4
Ln([C])
130
230
330
430
530
630
730
830
930
1030
t (min)

Figure S11. Stacked ^{1}H NMR spectra at 353K.

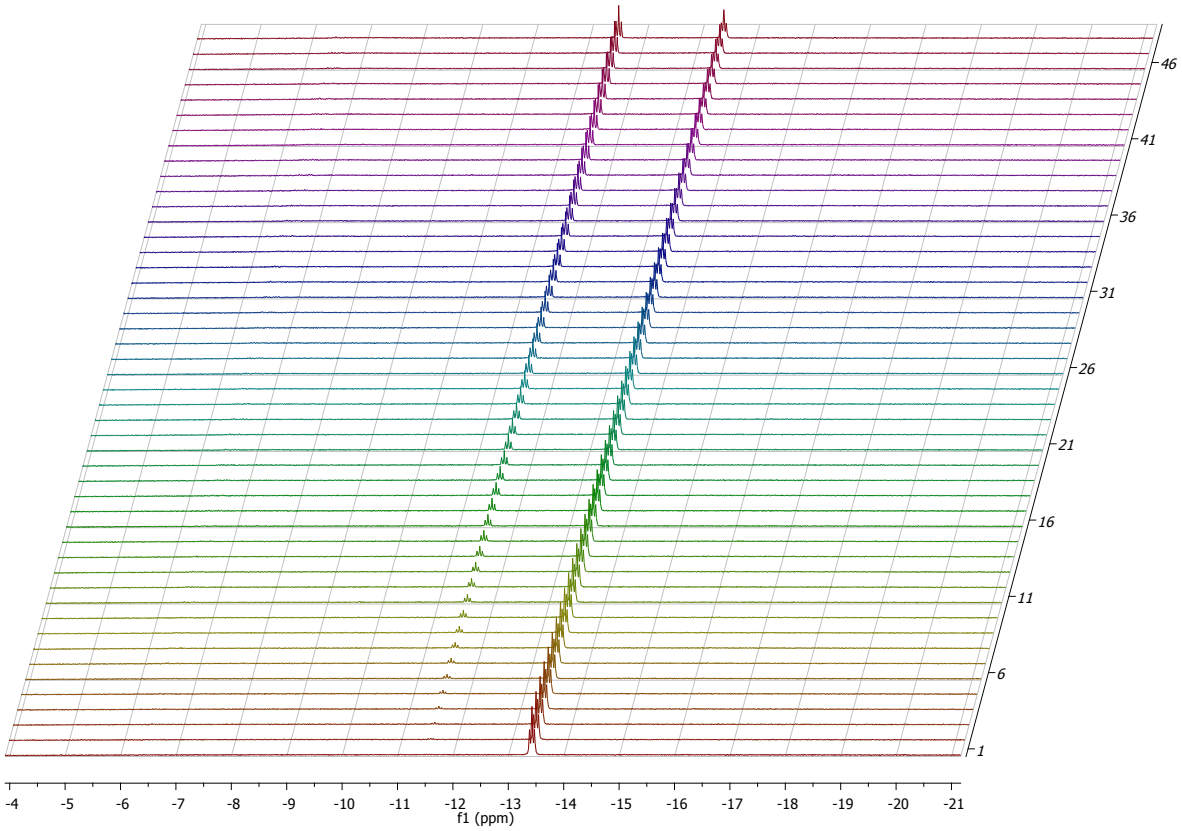

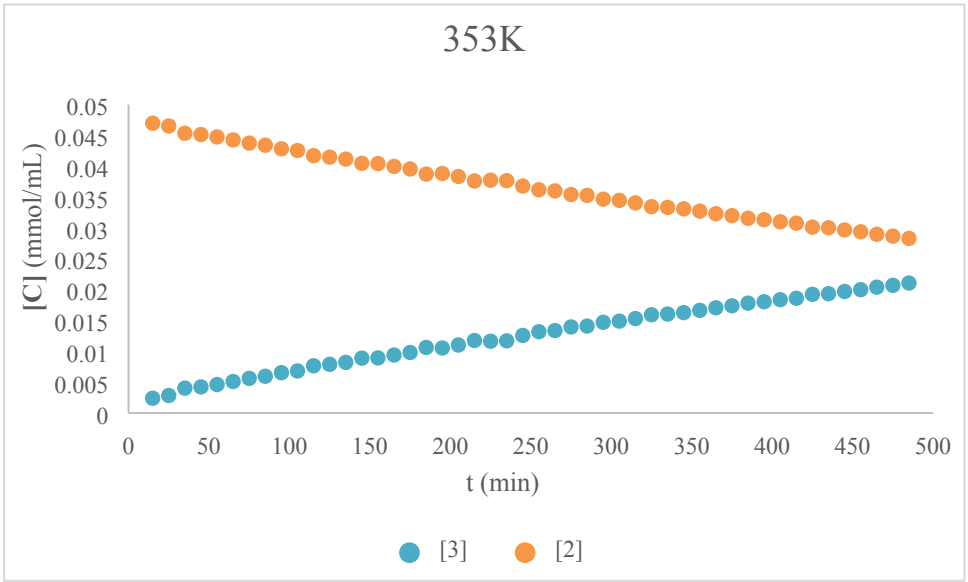

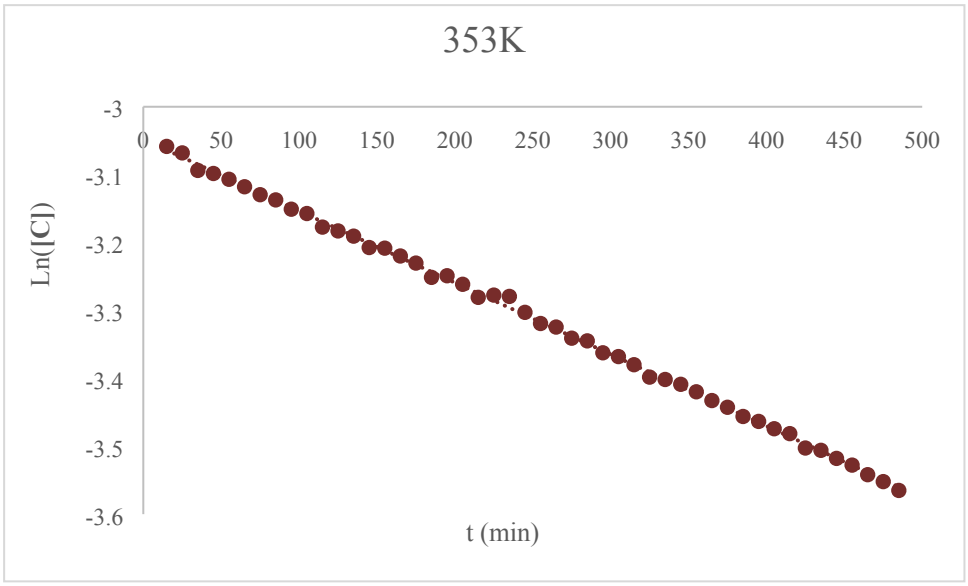
353K
-3
-3.1
-3.2
-3.3
-3.4
-3.5
-3.6
Ln([C])
0
50
100
150
200
250
300
350
400
450
500
t (min)

Figure S12. Stacked ^{1}H NMR spectra at 363K.

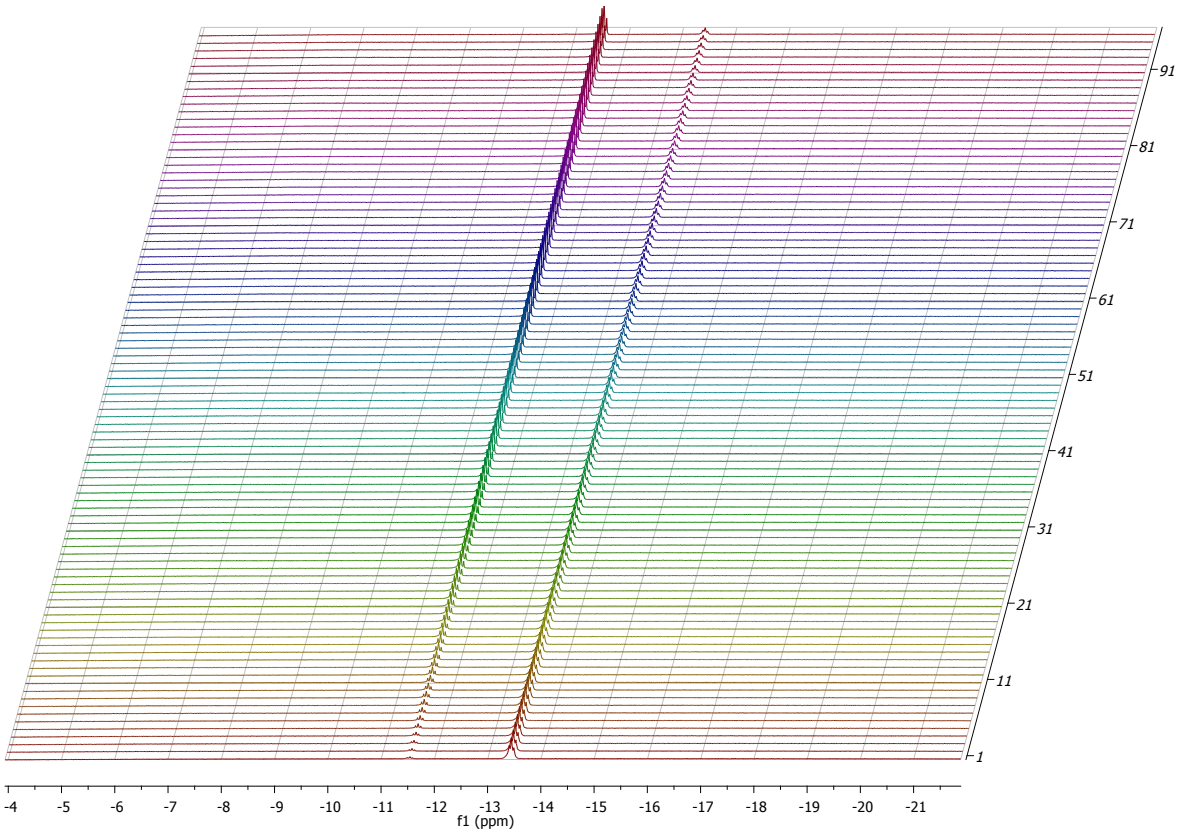

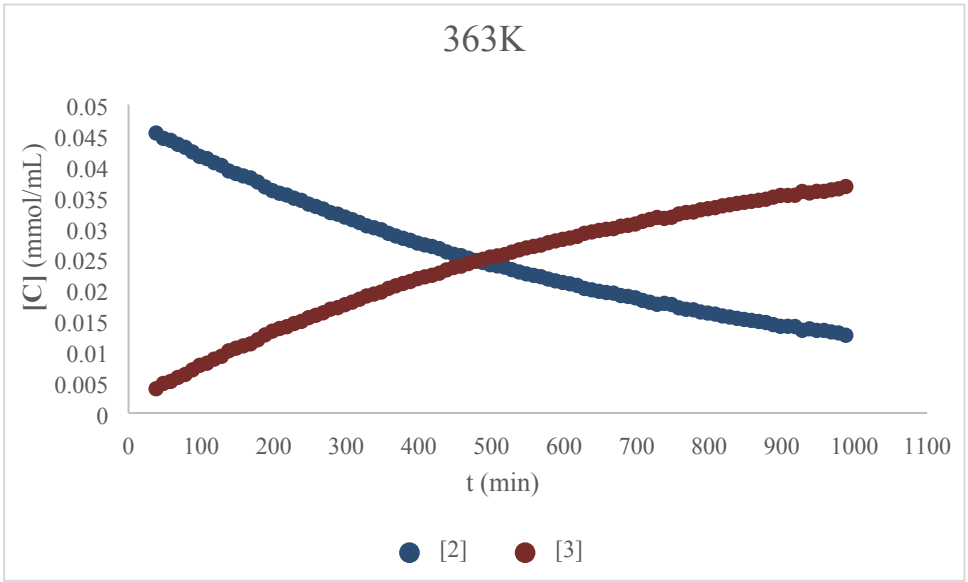

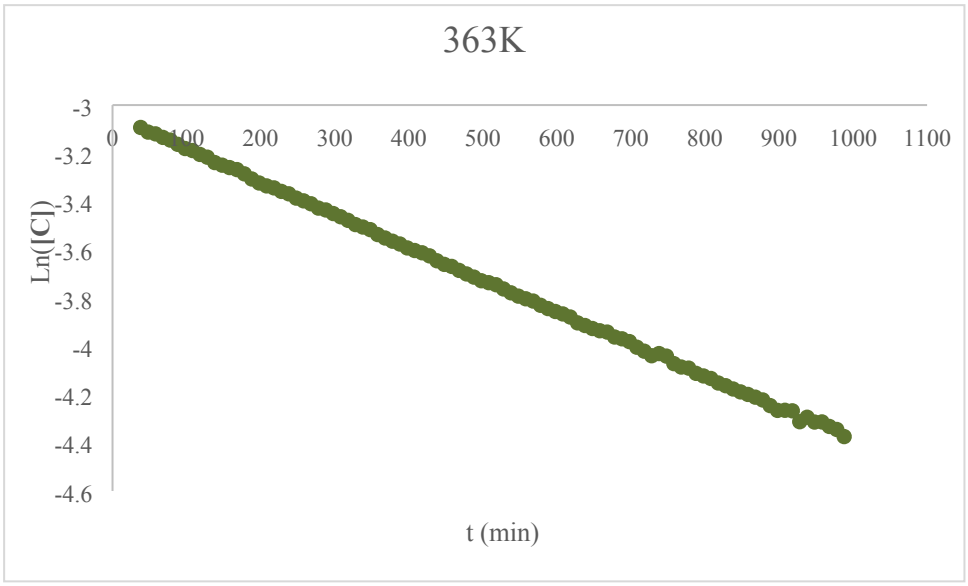
363K
-3
-3.2
-3.4
-3.6
-3.8
-4
-4.2
-4.4
-4.6
Ln([C])
0
100
200
300
400
500
600
700
800
900
1000
1100
t (min)

Figure S13. Stacked ^{1}H NMR spectra at 373K.

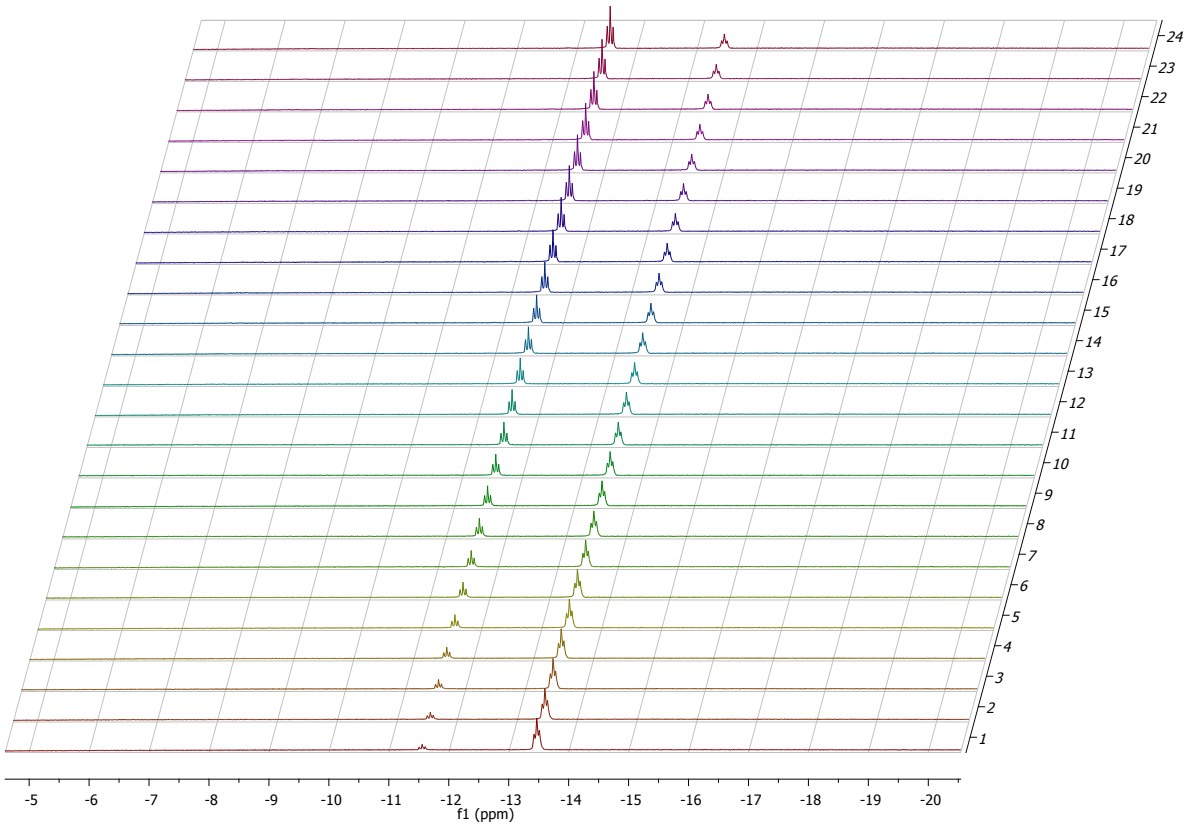

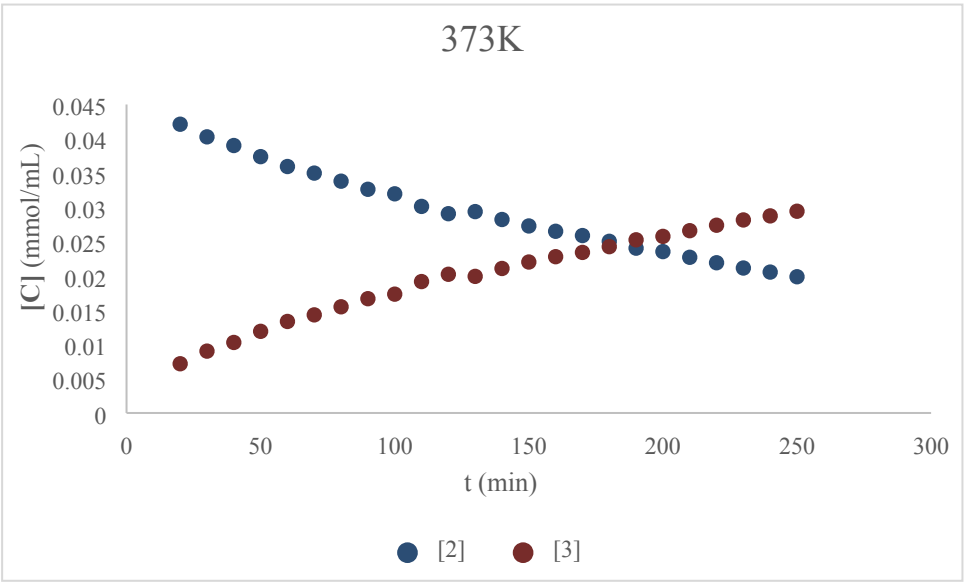

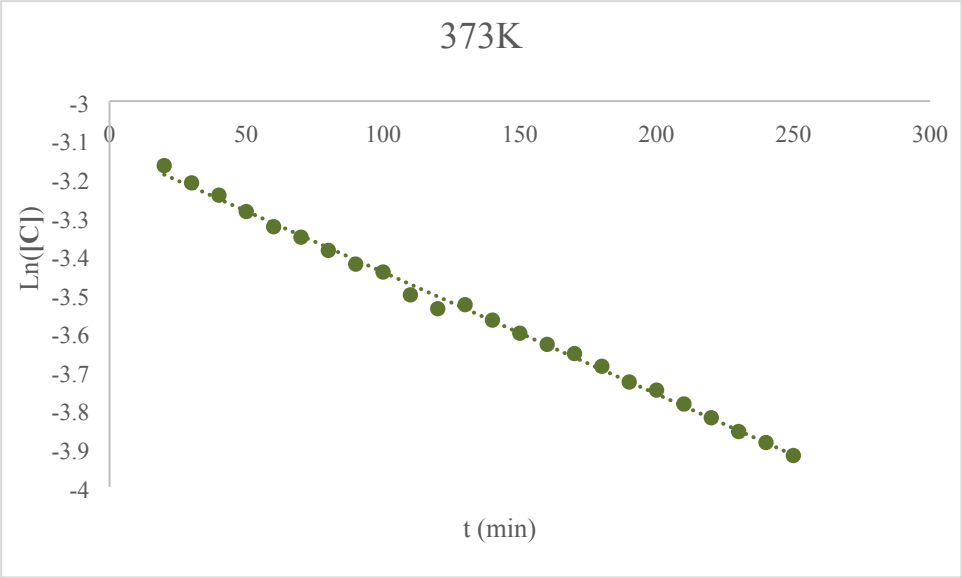

The influence of the temperature on the reaction rate was investigated in the temperature range 343-373 K and in C_7D_8 and at $[\mathbf{2}]_0$ =0.0493 mM. The rate constant was determined at four different temperatures and the overall activation parameter $\Delta H^{\neq}$ was determined using the logarithmic form of the Eyring equation.

$$\ln\left(\frac{k}{T}\right) = \ln\left(\frac{k_b}{h}\right) + \frac{\Delta S^{\neq}}{R} - \frac{\Delta H^{\neq}}{RT}$$

T (K)	1/T (K^{-1})	k_{obs} (min^{-1})	k_{obs} (s^{-1})	k_{obs}/T ($s^{-1}.K^{-1}$)	$Ln(k_{obs}/T)$
373	0,00268097	0,0032	5,33333E-05	1,4298E-07	-15,760527
363	0,00275482	0,0014	2,33333E-05	6,4279E-08	-16,56003
353	0,00283286	0,0011	1,83333E-05	5,1936E-08	-16,773258
343	0,00291545	0,0004	6,66667E-06	1,9436E-08	-17,756121

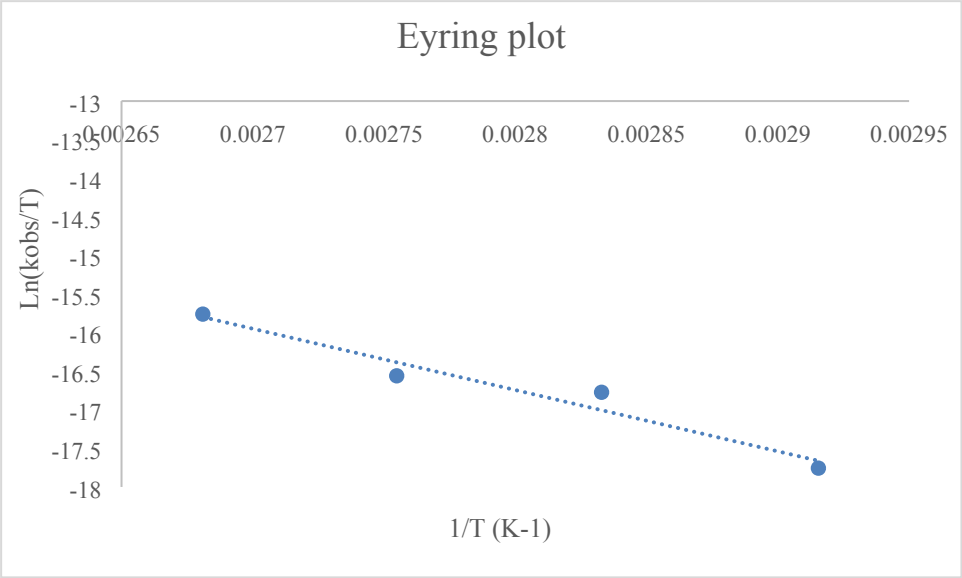

$\Delta H^{\#}$ = 7942.4 x 8.31 = 66.0 kJ.mol^{-1}.

3. ^{1}H NMR spectra of catalytic reaction solutions.

Figure S14. Hydrogenation of methyl heptanoate.

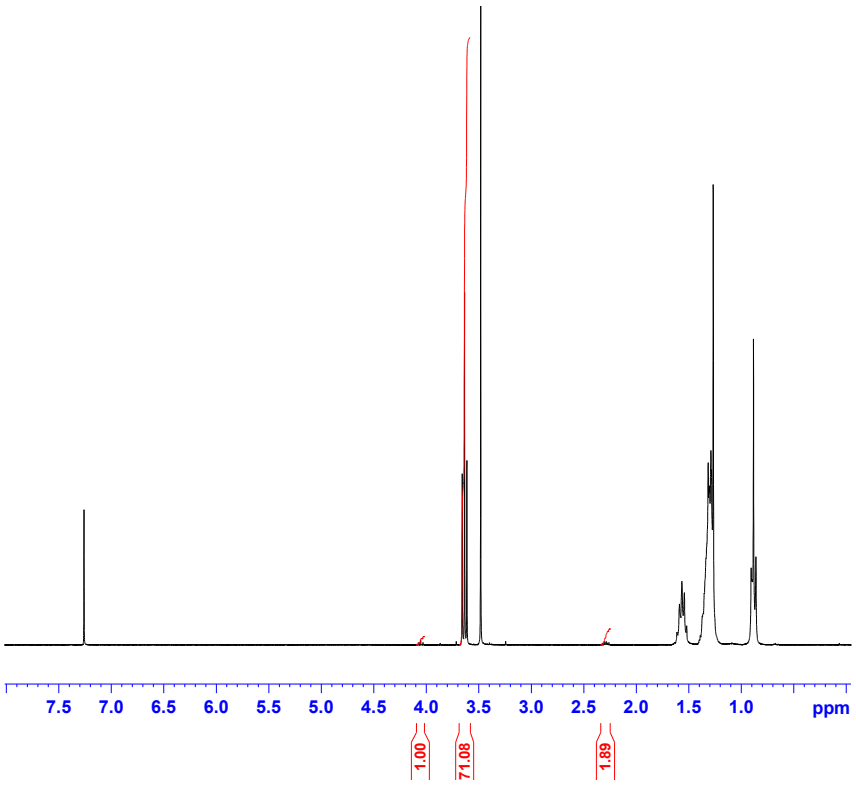

Figure S15. Hydrogenation of methyl heptanoate followed by dehydrogenation sequence.

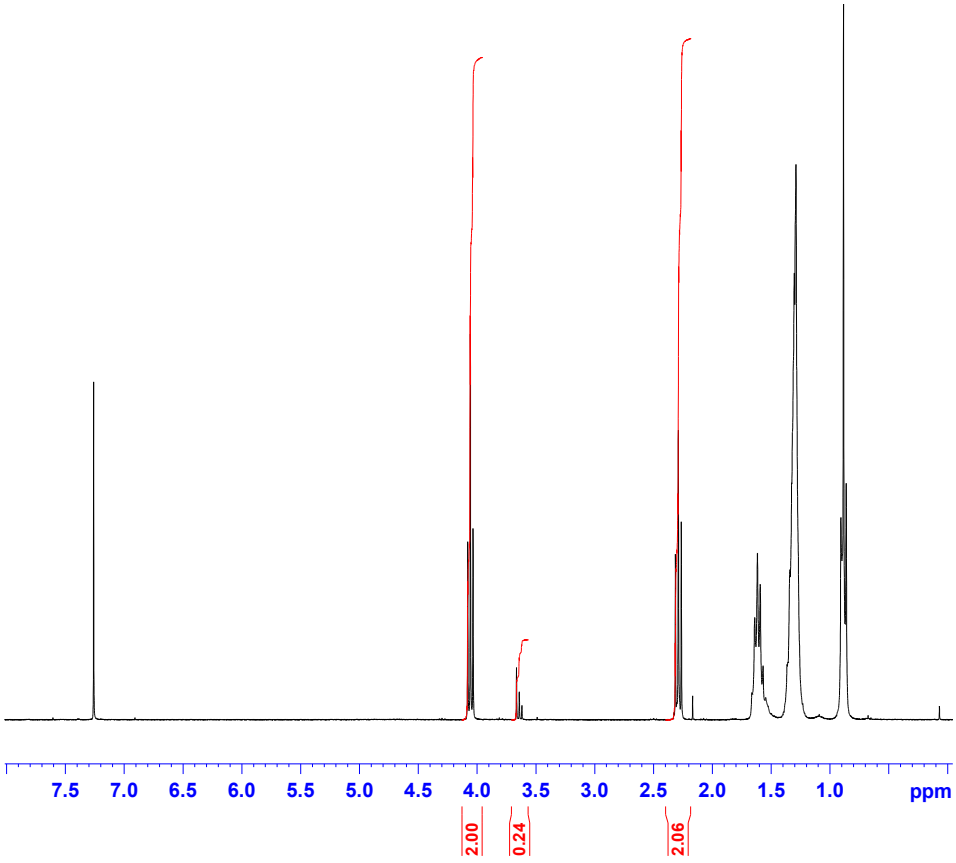

Figure S16. Hydrogenation of methyl oleate

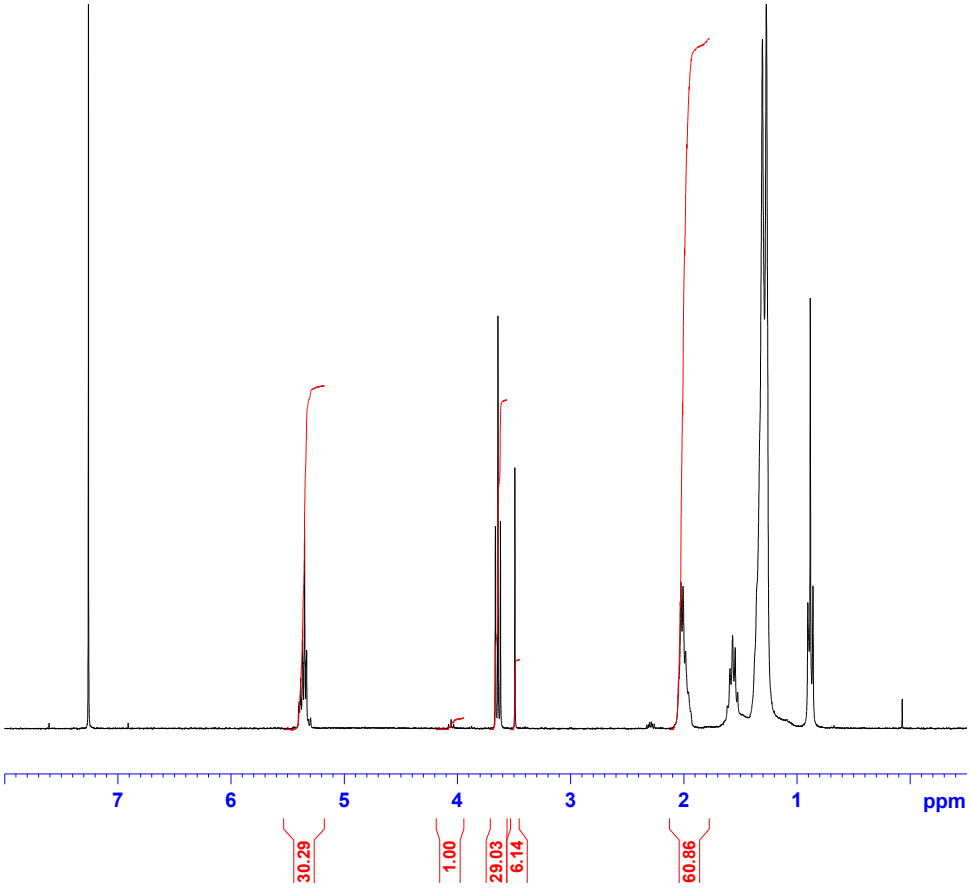

Figure S17. Hydrogenation of methyl oleate followed by dehydrogenation sequence.

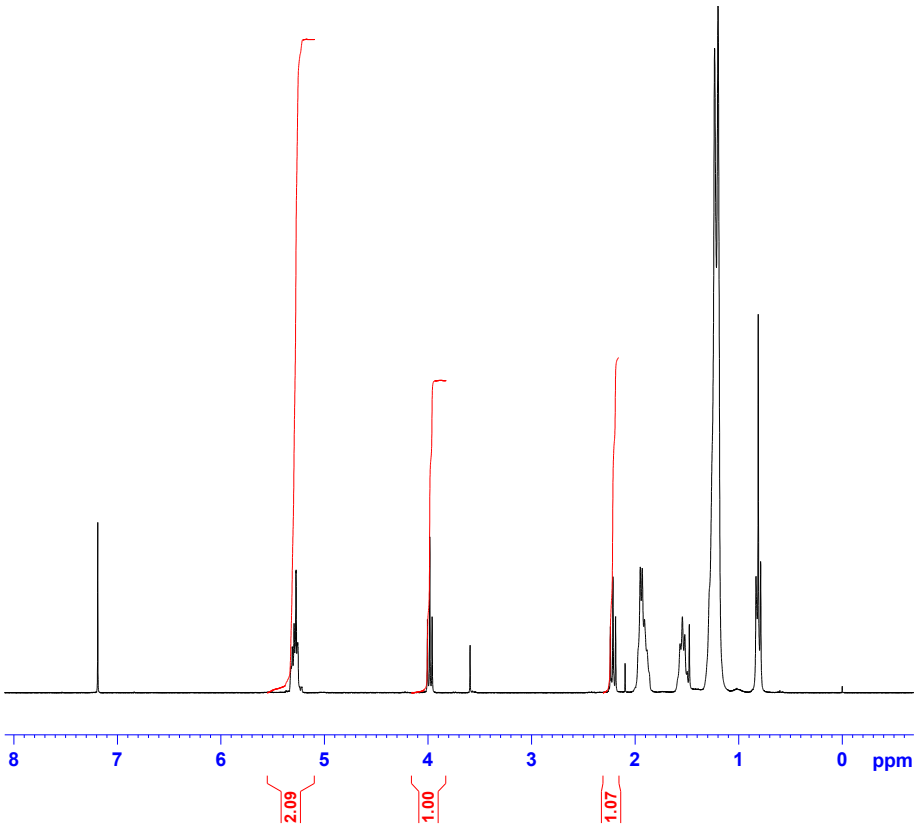

4. Physico-chemical property measurements.

Figure S18. TGA diagram of heptyl heptanoate.

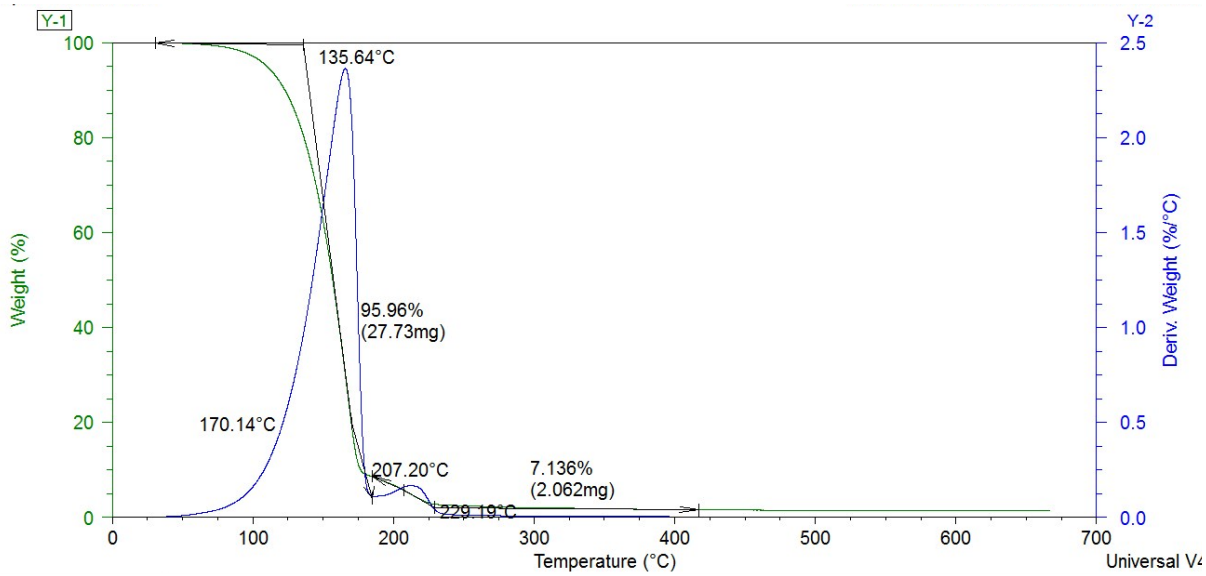

Figure S19. TGA diagram of oleyl oleate.

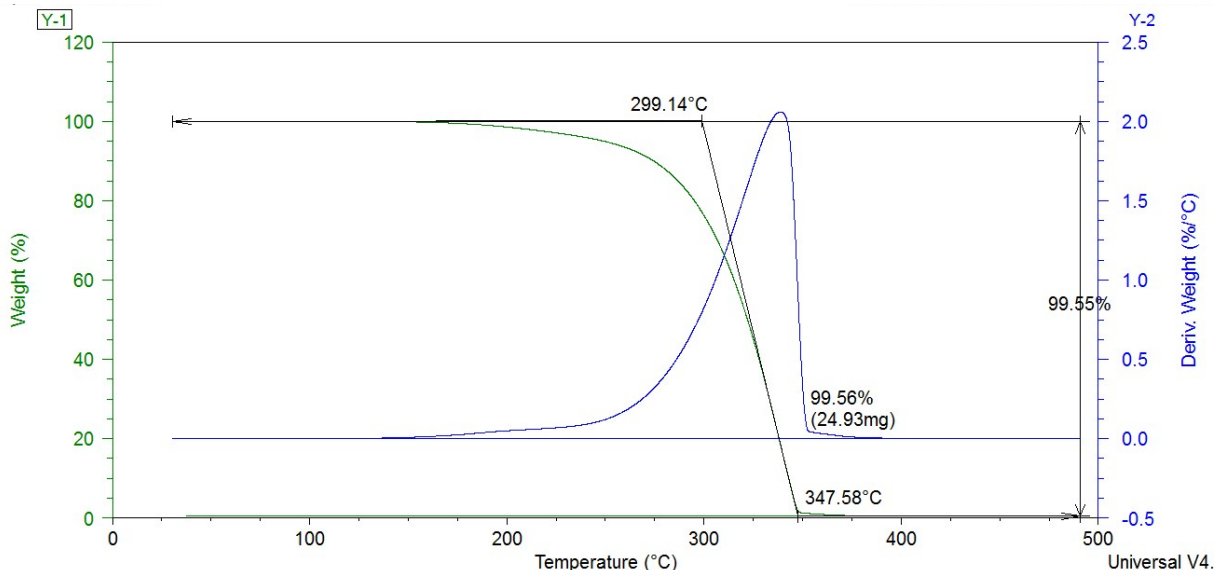

Figure S20. TGA diagram of wax esters produced from RADIA 7060.

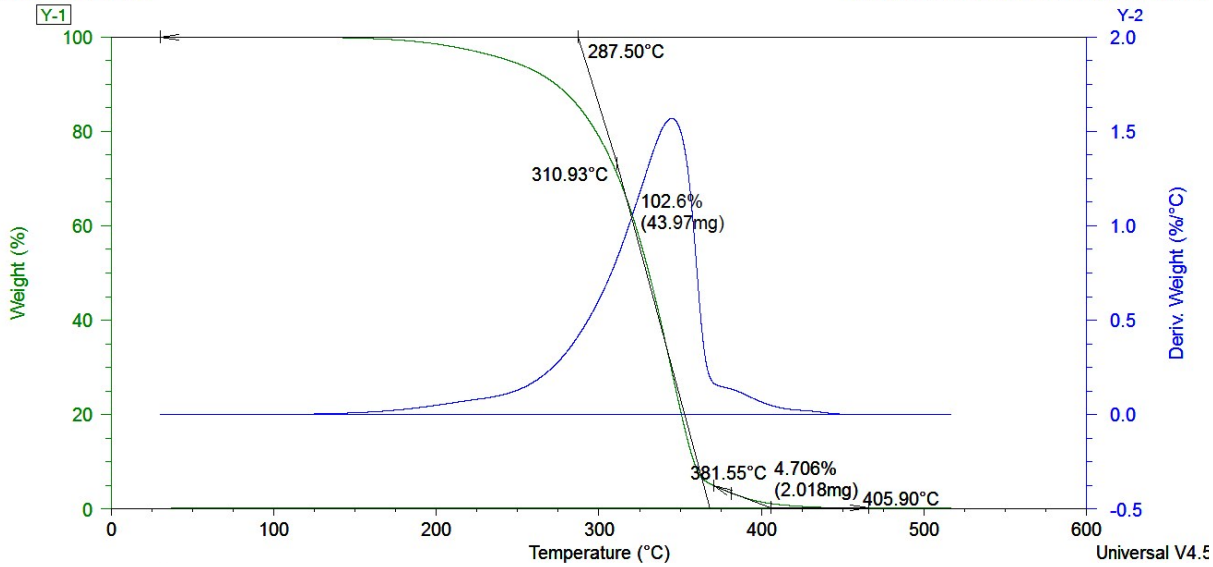

Figure S21. TGA diagram of Jojoba oil.

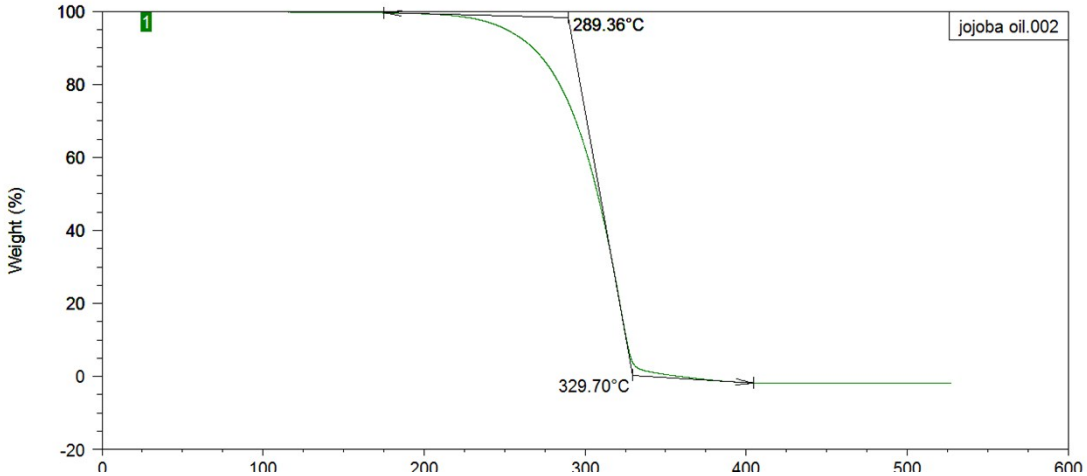

Figure S22. DSC diagram of heptyl heptanoate.

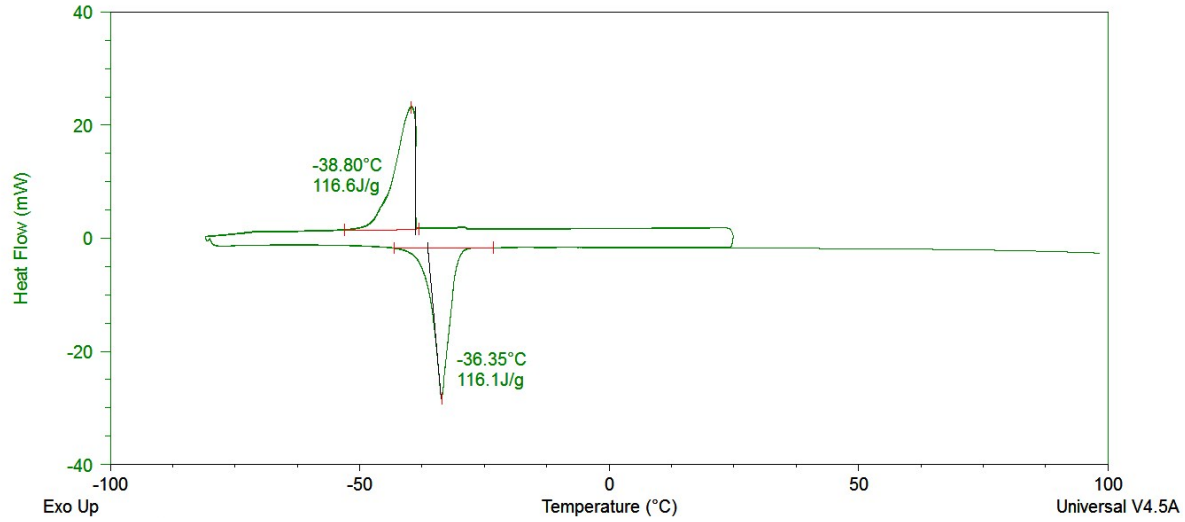

Figure S23. DSC diagram of oleyl oleate.

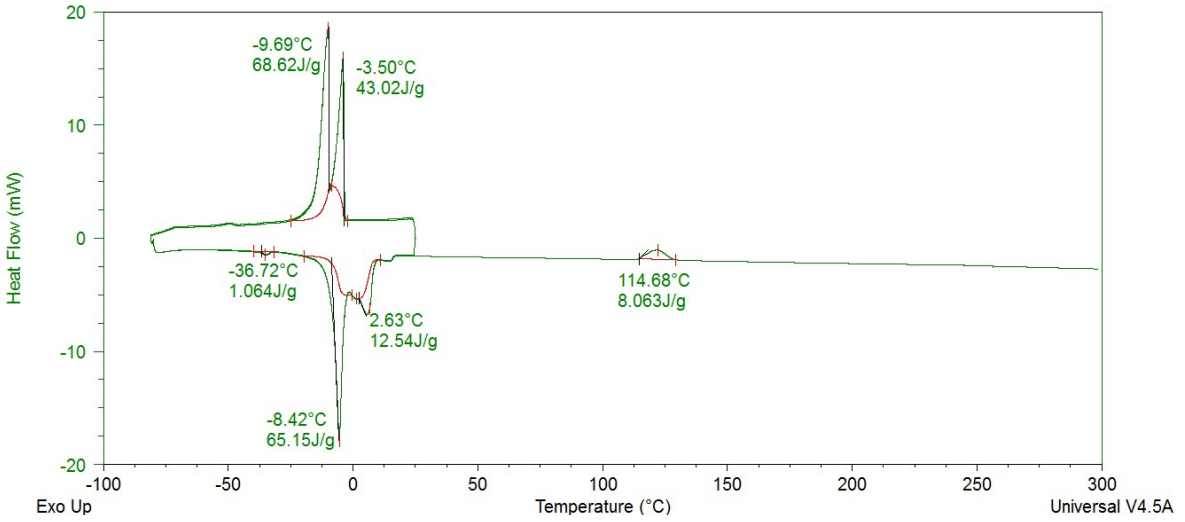

Figure S24. DSC diagram of wax esters produced from RADIA 7060.

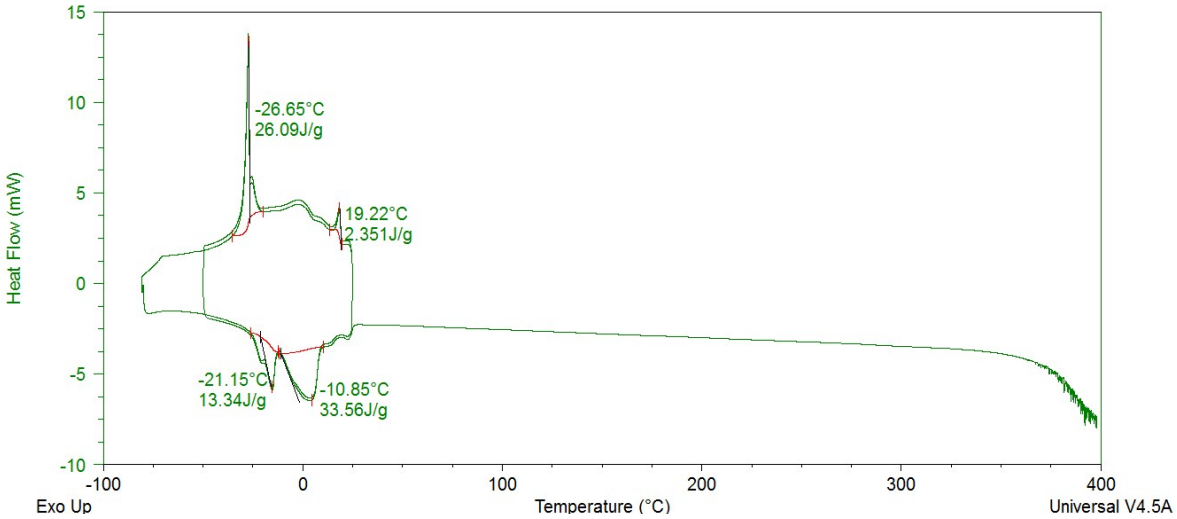

Figure S25. DSC diagram of Jojoba oil.